

Trained Artificial Neuron-Based Intelligent Speed Controller for Interior Permanent Magnet Synchronous Motor

T.NIRMAL KUMAR¹, S.PRABHAKARAN².

¹ Post Graduate Student, The Kavery Engineering College, Salem, India.

² Asst Professor, The Kavery Engineering College, Salem, India.

Email: nirmalkumarr01@gmail.com

Abstract-This paper presents a speed control of interior permanent magnet synchronous motor (IPMSM) simplified by single artificial neuron(SAN). Conventional artificial neural network(ANN) based motor controller requires widespread offline training, in which both time consuming and widespread knowledge of motor performance of specific drive system. And at the same time drive performance is unpredictable when the parameters outside the training sets are encountered. In the proposed drive system overcomes these confines by requiring no offline training and it is robust under varying parameters, and easily adaptable to different drive system.

Keywords:- Artificial neural network(ANN), intelligent control, Interior permanent synchronous motor(IPMSM), motor control.

1. INTRODUCTION

The interior permanent magnet synchronous motor in speed controlled high performance drive applications is required to quickly achieve the command speed and maintains that operating point with maximum accuracy and minimal perturbation despite the application of sudden and unknown disturbances.

Conventionally, proportional integral(PI) and proportional integral derivative(PID) speed controllers haven utilized to meet this control challenges. The operation of the IPMSM strongly affected by rotor magnetic saliency, saturation and armature reaction effects with ANN to tune PI controller parameters to achieve greater insensitivity to load and parameter variations. A downside of ANN-based drive systems to date is that they require extensive offline training and can react unpredictably when encountering operating conditions outside their original training sets. This paper presents an ANN-based controller for the IPMSM drive which requires minimal offline training yet precisely and accurately follows command speed with insensitivity to load and parameter variations. The system is simplified to a single artificial neuron (SAN) to minimize complexity and computational burden requirements. Speed error is conditionally used at each iteration adaptively modify the SAN parameters to produce the precise command torque to minimize speed error. To ensure drive stability, further tuning is conditionally executed at each iteration by the comparison of the

SAN's output command torque to a reference command torque.

Approximations of the maximum torque per ampere (MTPA) and field weakening (FW) modes of operation are incorporated, resulting in efficient operation over the drive's entire speed range.

2. IPMSM DYNAMICS

Adopting the conventional practice of neglecting iron losses, the mathematical model of an IPMSM drive can be described by the following equations in a synchronously rotating rotor $d-q$ reference frame as

$$\begin{bmatrix} v_q \\ v_d \end{bmatrix} = r_s \begin{bmatrix} i_q \\ i_d \end{bmatrix} + \begin{bmatrix} pL_q & P\omega_r L_d \\ -P\omega_r L_q & pL_d \end{bmatrix} \times \begin{bmatrix} i_q \\ i_d \end{bmatrix} + \begin{bmatrix} P\omega_r \psi_f \\ 0 \end{bmatrix} \quad (1)$$

$$T_e = T_l + B_m \omega_r + J_m p \omega_r \quad (2)$$

$$T_e = \frac{3P}{2} [\psi_f i_q + (L_d - L_q) i_d i_q] \quad (3)$$

3. CONTROL ALGORITHM

The torque equation(3) indicates that there exists a nonlinear relationship between the electrical torque and d -axis and q -axis currents. In order to incorporate this nonlinearity in a practical IPMSM drive, a control technique known as MTPA is derived which provides maximum motor torque with the minimum possible

stator current for operation below base speed for extended speed operation, FW mode is utilized.

3.1 MTPA MODE

The maximum torque per unit current can be achieved by differentiating torque equation with respect to q -axis current i_q and setting the resulting equation to zero, which gives

$$i_d = \frac{\psi_f}{2(L_q - L_d)} - \sqrt{\frac{\psi_f^2}{4(L_q - L_d)^2} + i_q^2} \quad (4)$$

Substituting (4) into (3), one can get a nonlinear relationship between i_q and T_e as

$$T_e = \frac{3P}{2} \left(\psi_f i_q - \frac{\psi_f i_q}{2} - (L_d - L_q) \sqrt{\frac{\psi_f^2 i_q^2}{4(L_q - L_d)^2} + i_q^4} \right) \quad (5)$$

In real time, the implementation of driven system becomes potentially undefined and computationally burdensome with expressions i_d and T_e . The d - and q -axis currents are obtained by expanding the square root term of i_d via a Taylor series expansion about zero, giving

$$i_d = -0.11825 i_q^2 \quad (6)$$

Equation (6) is obtained using the motor parameters. By substituting (6) into (3), the following relationship can be obtained

$$i_q = -1.06157 T_e \quad (7)$$

Equations (6) and (7) are used for the approximate MTPA control of the IPMSM

3.2 FW MODE

In the extended speed range, which is roughly above the base value and where the magnet-generated back electromotive force causes a reduction in torque capacity, the FW mode of operation is used to generate the appropriate command currents. In the FW scheme, the d - and q -axis components of phase current are constrained to maintain phase voltage at an optimum value with rated phase voltage set as maximum

$$V_o = \sqrt{v_d^2 + v_q^2} \leq V_{om} \quad (8)$$

Where V_{om} is the maximum operating phase voltage magnitude. Under the assumption of steady state, the d - q -axis model given in (1) is refined as

$$\begin{bmatrix} v_q \\ v_d \end{bmatrix} = \begin{bmatrix} 0 & P\omega_r L_d \\ -P\omega_r L_q & 0 \end{bmatrix} \begin{bmatrix} i_q \\ i_d \end{bmatrix} + \begin{bmatrix} P\omega_r \psi_f \\ 0 \end{bmatrix} \quad (9)$$

$$V_{om} = V_{am} - r_s I_{am} \quad (10)$$

$$i_d = -\frac{\psi_f}{L_d} + \sqrt{\frac{v_q^2}{P^2 \omega_r^2 L_d^2}} \quad (11)$$

Solving (8) for V_o gives,

$$v_q^2 = V_o^2 - v_d^2 \quad (12)$$

Substituting (12) into (11) results in the following equation i_d

$$i_d = -\frac{\psi_f}{L_d} + \frac{1}{L_d} \sqrt{\frac{V_o^2}{P^2 \omega_r^2} - L_q^2 i_q^2} \quad (13)$$

Substituting motor parameters into (13) gives

$$i_d = -7.39868 + \frac{1}{0.08488} \sqrt{\frac{V_o^2}{\omega_r^2} - 0.006331 i_q^2} \quad (14)$$

Expanding (14) in a Taylor series about $i_q=0$ and neglecting higher terms give

$$i_d = -7.39868 + \frac{11.7813}{\omega_r} V_o \quad (15)$$

Where

$$V_o \leq V_{om} = V_{am} - r_s I_{am}$$

Substituting (15) into (3) with the appropriate experimental machine parameters and solving for i_q give

$$i_q = \frac{T_e}{1.76614 - \frac{1.31232}{\omega_r} V_o} \quad (16)$$

3.3 CONTROL SCHEME LAYOUT

The block diagram shows the control scheme of the motor drive. The command torque $T_e^*(n)$ is obtained from SAN-based speed controller. Then using (7) or (16) the reference q -axis current i_q^* is computed from $T_e^*(n)$ subsequently. The reference d -axis i_d^* is calculated using (6) or (15), depending on the modes of operation. The corresponding three phase currents are determined by vector rotation. A hysteresis current controller compares the reference three-phase currents with actual currents and generates gate signals for the transistorized inverter.

The actual motor currents are measured by Hall-effect sensors which. Three phase reference q -axis and d -axis currents and rotor position angle obtained through an encoder mounted on the shaft of the motor. Computed three phase reference currents are converted to upper and lower hysteresis by adding and subtracting a preselected percentage band. Actual motor currents are compared to these hysteresis current limits and PWM gate drive signals generated accordingly.

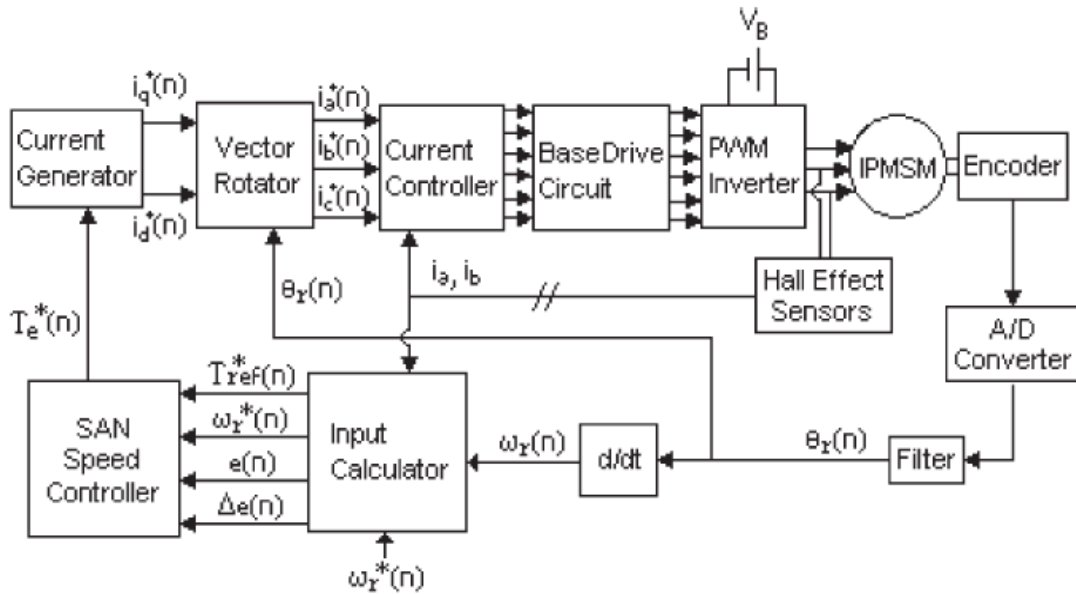


Figure.1 Block Diagram of SAN speed controller

4. DESIGN OF SAN CONTROLLER FOR IPMSM

4.1 SAN CONTROL PRINCIPLE

The dynamic model of the IPMSM can be rewritten from equation (1) and (2)

$$L_q p i_q + P \omega_r L_d i_d = v_q - r_s i_q - P \omega_r \psi_f \quad (17)$$

$$p \omega_r = (T_e - T_L - B_m \omega_r) / J_m \quad (18)$$

The load will be considered as having unknown nonlinear mechanical characteristics and can be modeled using the following equation as

$$T_L = A \omega_r^2 + B \omega_r + C \quad (19)$$

Where A , B , and C are arbitrary constants. To make the control task easier, the equations of an IPMSM are expressed as a single-input/single-output system by combining (18) and (19) in continuous time domain form as

A small increment ΔT_e in T_e causes a small increment $\Delta \omega_r$ in ω_r

$$J_m \frac{d\omega_r}{dt} = T_e - (B_m + B) \omega_r - A \omega_r^2 - C \quad (20)$$

$$J_m \frac{d(\omega_r + \Delta \omega_r)}{dt} = (T_e + \Delta T_e) - (B_m + B)(\omega_r + \Delta \omega_r) - A(\omega_r + \Delta \omega_r)^2 - C \quad (21)$$

Subtracting (20) from (21) gives,

$$J_m \frac{d(\Delta \omega_r)}{dt} = \Delta T_e - (B_m + B + 2A\omega_r)(\Delta \omega_r) - A(\Delta \omega_r)^2 \quad (22)$$

By replacing all the continuous quantities of (22) by their finite differences, the discrete-time small signal model of the simplified IPMSM with nonlinear load can be given as

$$\Delta T_e(n) = \frac{J_m}{t_s} \Delta e(n) + (B_m + B + 2A\omega_r(n)) \times \Delta \omega_r(n) + A \{ \Delta \omega_r(n) \}^2 \quad (23)$$

Hence

$$T_e^*(n) = \int_{\text{discrete}} \Delta T_e(n) = f(\Delta e(n), \Delta \omega_r(n), \omega_r^*(n)) \quad (24)$$

Thus, the purpose of using the SAN speed controller is to obtain the command torque by mapping the nonlinear functional relationship between command electrical torque T_e and rotor command speed ω_r , speed error $e(n)$, and change in speed error $\Delta e(n)$, with no reliance on knowledge of motor parameters

4.2 REFERENCE COMMAND TORQUE

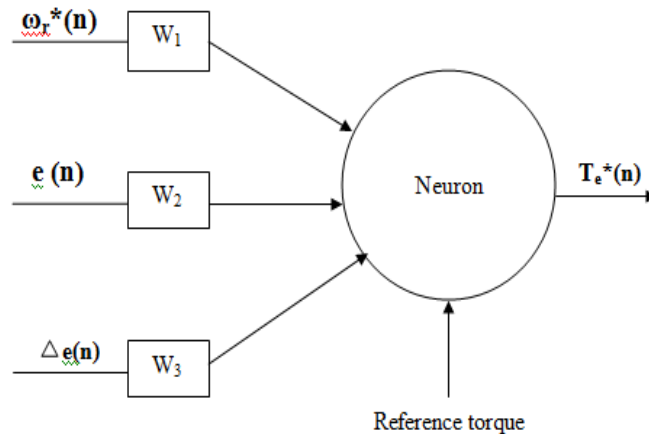


Figure.2 Single Artificial Neuron

Equation (2) can be rearranged and discretized to give

$$T_L(n) = T_e(n) - J_m p\omega_r(n) - B_m\omega_r(n). \quad (25)$$

Since J_m and B_m are known, $\omega_r(n)$, the present sample of rotor speed, can be obtained from a position sensor mounted to the rotor shaft, and $p\omega_r(n) = (\omega_r(n) - \omega_r(n-1))/t_s$ is the change in rotor speed over the sampling period, load torque $T_L(n)$ —at the present sample can be calculated directly from (25) if $T_e(n)$ is known at that sampling instant $T_e(n)$ can be calculated

From (3) as

$$T_e(n) = \frac{3P}{2} [\psi_f i_q(n) + (L_d - L_q) i_d(n) i_q(n)] \quad (26)$$

i'_d and i'_q can be calculated via Park's equation and reference frame transformation from samples of $i_a(n)$, $i_b(n)$, and $i_c(n)$ taken by current sensors. P and ψ_f are known, and L_d and L_q must be assumed to have known values.

With the current sample value of T_L now having been calculated, can be utilized to calculate the reference command torque as follows

$$T_{ref}^*(n) = J_m p\omega_r(n) + B_m\omega_r(n) + T_L(n). \quad (27)$$

This value of command torque is calculated with the assumption that L_d and L_q have constant known values. That assumption is incorrect. Using the actual inductance curves of our test motor indicates that this T_{ref} command may vary from the correct torque value by up to several value at the most extreme cases. This command torque, however, merely serves as a reference for the real-time training of the SAN and to set bounds to assure drive stability and for these purposes it is sufficient To

reduce computational burden the artificial neural network is simplified by single artificial neuron(SAN) that was shown in figure (2). To minimize computational burden, a single feed forward neuron structure is employed, with command torque being the only output of the SAN controller. Inputs to the SAN are the present sample of command speed $r(n)$, present sample of speed error $e(n) = \omega_r^*(n) - \omega_r(n)$ and present sample of change of speed error $\Delta e(n) = \Delta\omega_r(n) - \Delta\omega_r(n-1)$. Neuron output ranges from -1 to 1 via a tan-sigmoid transfer function, so this value is multiplied by the maximum peak torque rating of the motor to obtain the actual torque command. Due to space limitations, the equations of the ANN structure are not included here—they are based directly on conventional feed forward ANN methods. The SAN structure is illustrated in figure 2.

Each iteration of combined speed- and T_{ref} -based training of the SAN-based controller imposes and 16 exponential operations. This is a significant increase and decrease in computational burden as compared to a single iteration of a conventional PID controller but only occurs when retraining is necessary. In real-world implementation on the laboratory equipment, the SAN-based drive was found to perform best at a maximum sampling rate of 5 kHz, whereas a typical PID-based controller could be sampled at 10 kHz. A more complex four-neuron-based ANN controller required the sampling.

From this command torque, the MTPA or FW approximations are used, as appropriate, to obtain the appropriate q - and d -axis command currents i_q and i_d respectively, to produce the desired motor speed. From these currents, the phase command currents, i_a , i_b , i_c are calculated and applied to the motor through the voltage-source inverter by a hysteresis controller.

In order to provide adaptive control, the weights and bias of the SAN are updated, by back propagation, whenever the speed error exceeds an

appropriately chosen threshold. If this threshold is not exceeded, the weights and bias will be used again in the following iteration. The speed error itself $\omega_r^* - \omega_r(n)$ is used for back-propagation updating.

The learning rates of the SAN were tuned manually so that the SAN could train itself within the torque error boundary for all but four of the samples, where T^* ref was used as command torque. As the sampling rate was 5 kHz, this indicates that the SAN successfully provided the torque command for 4996 of the 5000 total torque commands issued.

5. SIMULATION AND RESULTS

The proposed system is analyzed with the help of MATLAB software tools and the approximate results

for various values of rotor speed and current are represented in graphical form.

The complete 3phase IPMSM drive system has been implemented by simulation. The actual motor current was measured by Hall Effect sensors which are fed to controller board.

As the motor neutral is isolated, only two phase currents are fed back, and the other phase current is calculated from them. Three-phase reference currents are generated utilizing reference q - and d -axis currents and rotor position angle obtained through an encoder mounted on the shaft of the motor

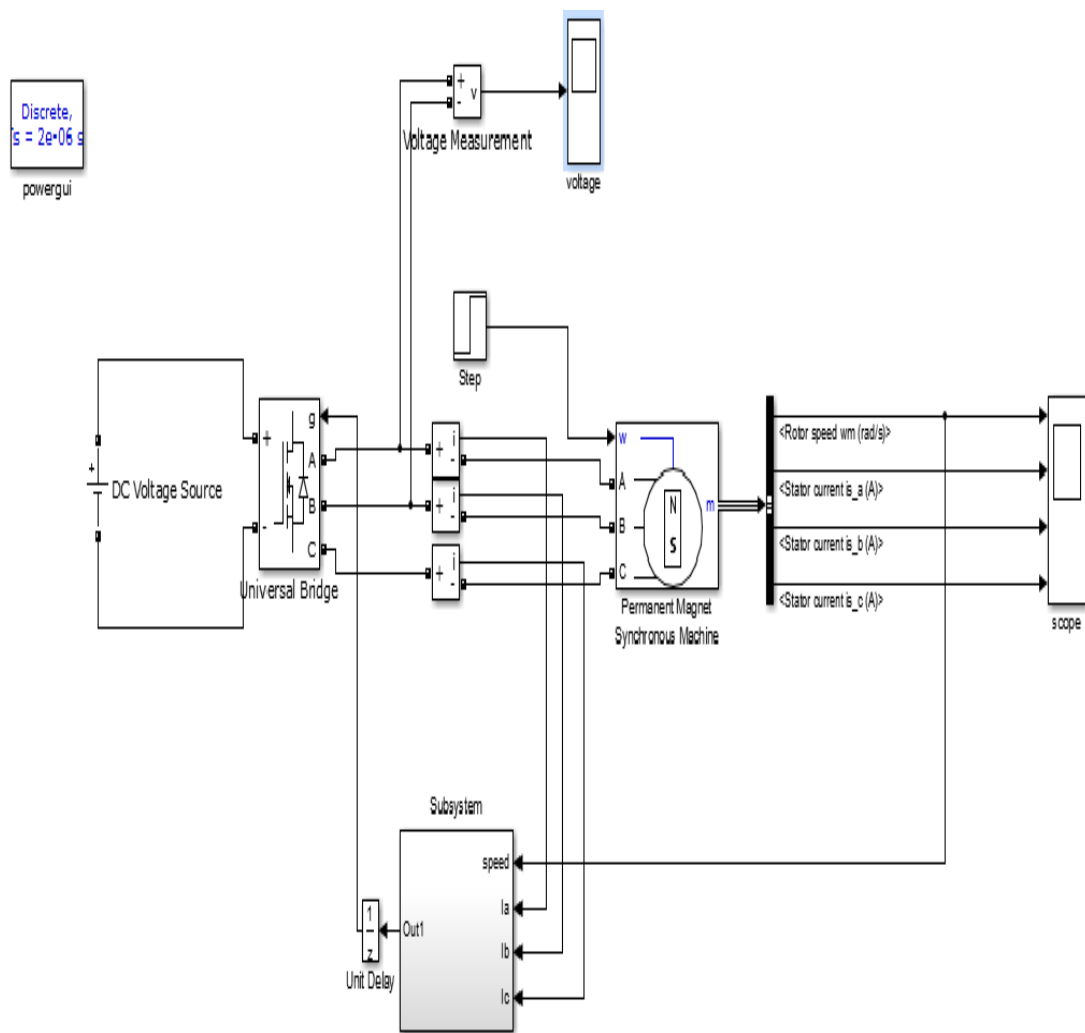


Figure.3 Simulation diagram of IPMSM speed controller

Output waveforms

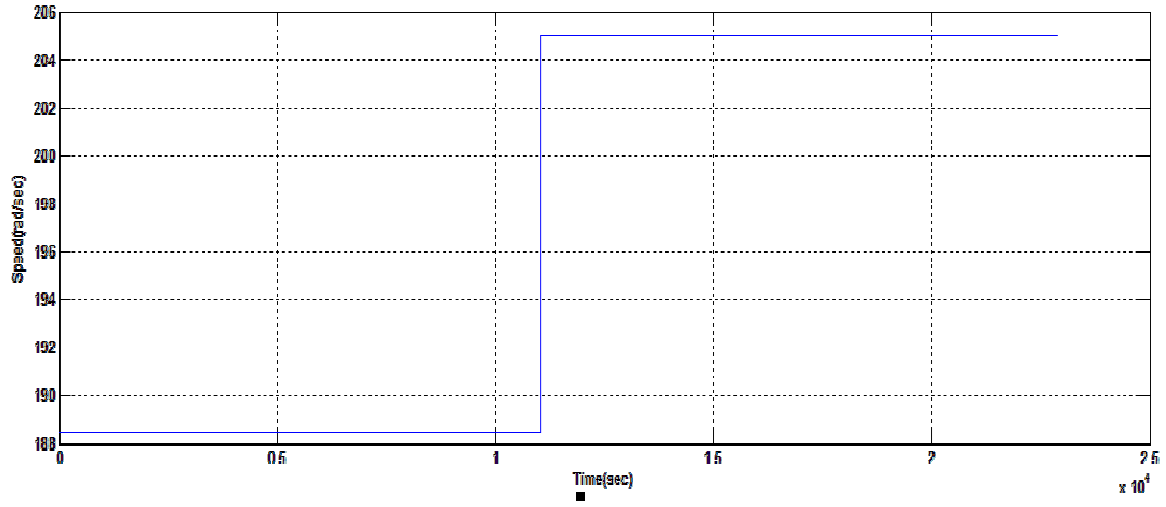
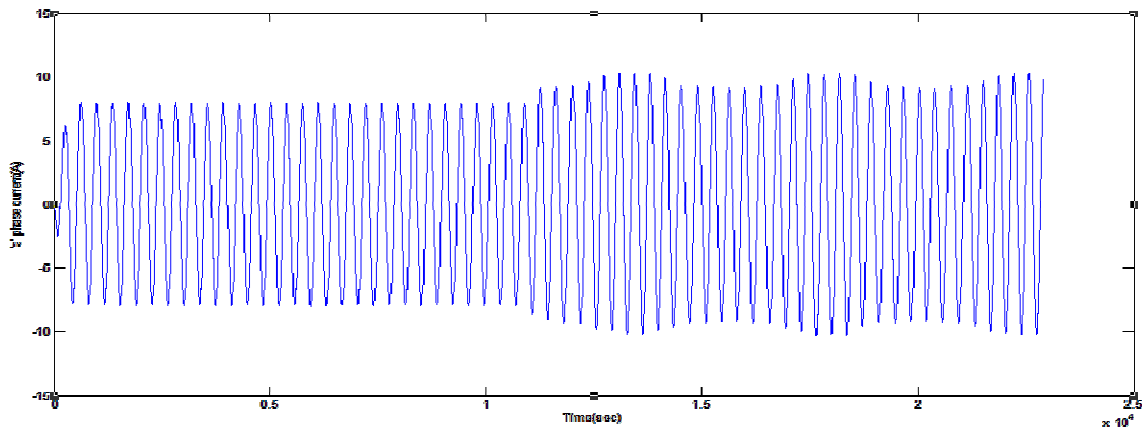
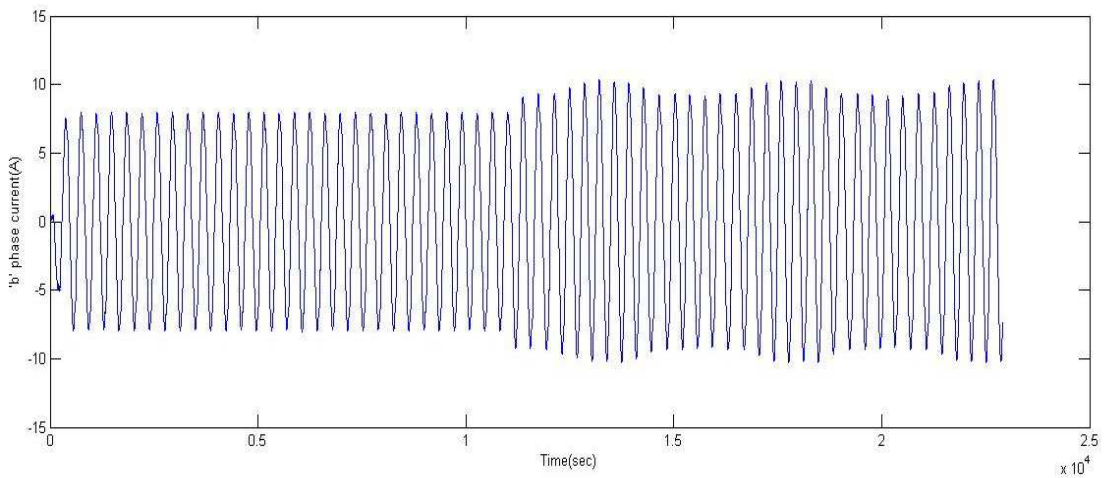


Figure.4 SimulatedRotor speed (rad/sec)



'a' phase current(A)



'b' phase current(A)

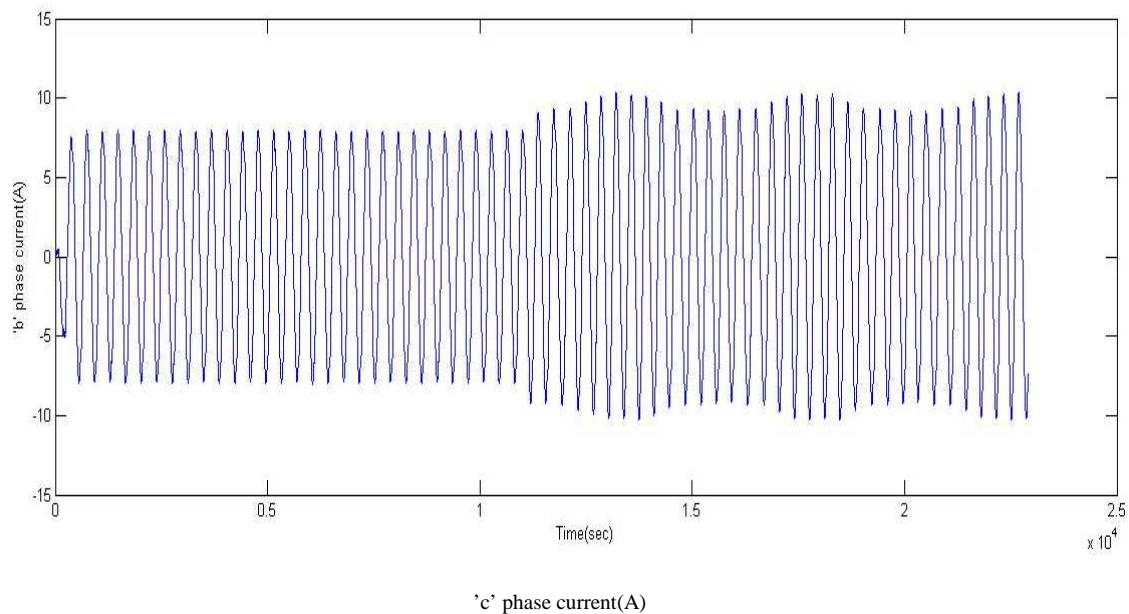


Figure.5 Simulated three phase currents

6. CONCLUSION

In this paper, the SAN-based speed controller with real-time training offers excellent speed response and load handling for high performance IPMSM drives. From all simulation and experimental results, it is clearly established that the SAN-based controller system provided superior real-time performances of the IPMSM motor drive over all operating speed ranges in comparison to those obtained under conventional PID control. The SAN-based real-time control strategy can be a good choice to provide adaptive control of the IPMSM drive without imposing a high computational burden or requiring extensive offline training.

MOTOR PARAMETERS

3 – Φ , 1 hp, 208 V, 60 Hz, $P = 2$, $L_d = 0.04244$ H, $L_q = 0.07957$ H, $r_s = 1.93$ Ω , $J_m = 0.003$ Kg \cdot m², $B_m = 0.0008$ N \cdot m/rad/s, and $\psi_f = 0.314$ V/rad/s.

References

- [1] B. K. Bose, "A high performance inverter-fed drive system of an interior permanent magnet synchronous machine," *IEEE Trans. Ind. Appl.*, vol. 24, no. 6, pp. 987–997, Nov./Dec. 1988.
- [2] C. B. Butt, M. A. Hoque, and M. A. Rahman, "Simplified fuzzy logic based MTPA speed control of IPMSM drive," *IEEE Trans. Ind. Appl.*, vol. 40, no. 6, pp. 1529–1535, Nov./Dec. 2004.
- [3] A. Consoli and Antonio, "A DSP based sliding mode field oriented control of an interior permanent magnet synchronous motor drive," in *Proc. IPEC Conf. Rec.*, Tokyo, Japan, 1990, pp. 263–303.

- [4] M. R. Emami, I. B. Turksen, and A. A. Goldenburg, "Development of a systematic methodology of fuzzy logic modeling," *IEEE Trans. Fuzzy Syst.*, vol. 6, no. 3, pp. 346–361, Aug. 1998

BIOGRAPHIES



Nirmal kumar.T He is pursuing M.E in Power Electronics and drives in The Kavery Engineering college. He completed B.E in Maharaja prithvi engineering college at 2008. His research is about speed control of IPMSM using trained ANN.



Prabhakaran.S He is working as Assistant professor in The kavery Enginerring college from 2011 to present. He completed M.Tech in B.S Abdur rahman university at 2011 and he completed B.E in Maha engineering college at 2009.